

## Supporting Information

# Bio-inspired Non-immunogenic Multifunctional Sealant for Efficient Blood Clotting and Suture Free Wound Closure

*Snehasish Ghosh,<sup>†1</sup> Paramita Gayen,<sup>†2</sup> Somnath Jan,<sup>2</sup> Anyam Vijay Kishore,<sup>5</sup> Vinod Kumar,<sup>5</sup> Argha M. Mallick,<sup>2</sup> Asmita Mukherjee,<sup>2</sup> Samit Kumar Nandi,<sup>\*5</sup> and Rituparna Sinha Roy<sup>\*2,3,4</sup>*

<sup>1</sup> Department of Chemical Sciences, <sup>2</sup> Department of Biological Sciences, <sup>3</sup> Centre for Advanced Functional Materials, <sup>4</sup> Centre for Climate and Environmental Studies, Indian Institute of Science Education and Research Kolkata, Mohanpur 741246, India.

<sup>5</sup> Department of Veterinary Surgery and Radiology, West Bengal University of Animal and Fishery Sciences, Kolkata – 700037, West Bengal, India.

<sup>†</sup> equal contribution

\*Corresponding Authors:

\***E-mail:** rituparna@iiserkol.ac.in (R.S.R.).

\***E-mail:** drsknandi@wbuafscs.ac.in (S.K.N).

**Figure S1.** MALDI-TOF mass spectra of sealant peptides.

**Figure S2.** CD spectra of sealant peptides in MeOH and pH 7.4 Tris. HCl buffer.

**Figure S3.** TEM and AFM images of peptide MP5.

**Figure S4.** TEM images of sealants 6-8 and nano-mechanical force of sealants 7 -8 obtained from AFM studies.

**Figure S5.** MALDI-TOF mass spectra of peptides 3 and MP5 in presence of mushroom tyrosinase enzyme.

**Figure S6.** Chemical structure of single and double tyrosine oxidation product of peptide MP5.

**Figure S7.** FE-SEM images of blood corpuscles with sealants 6-8. *Ex-vivo* clotting studies of fibrin and sealants 5-8.

**Figure S8.** Antibacterial activities of peptide 3 and sealant 5.

**Figure S9.** Semiquantitative analysis of histology data to determine the fold change of collagen deposition with respect to suture at day 7 and day 14

**Table S1.** Expected and observed mass values of peptides.

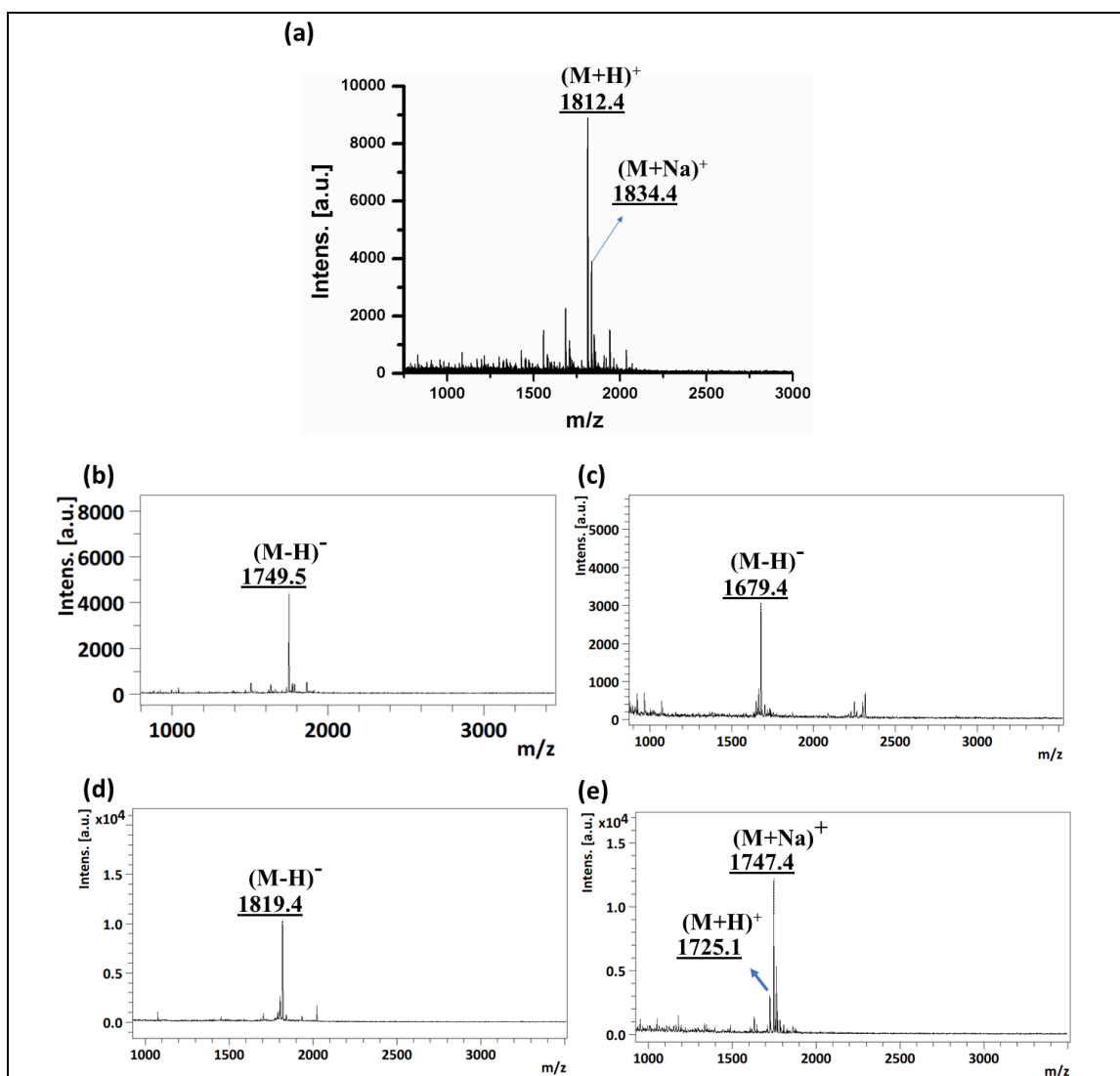


**Figure S1.** MALDI-TOF mass spectra of (a) peptide 3, (b) peptide MP5, (c) peptide MP6 (d) peptide MP7 and (e) peptide MP8.

Peptide 3 calculated mass: 1811.4 Da and Observed mass: 1812.4 Da (M+H)<sup>+</sup> and 1834.4 Da (M+Na)<sup>+</sup>.

Peptide MP5 calculated mass: 1750.6 Da and Observed mass: 1749.5 Da (M-H)<sup>-</sup>.

Peptide MP6 calculated mass: 1680.1 Da and Observed mass: 1679.4 Da (M-H)<sup>-</sup>.

Peptide MP7 calculated mass: 1820.3 Da and Observed mass: 1819.4 Da (M-H)<sup>-</sup>.

Peptide MP8 calculated mass: 1724.1 Da and Observed mass: 1725.1 Da (M+H)<sup>+</sup> and 1747.4 Da (M+Na)<sup>+</sup>.

**Table S1.** Peptide sequences and their mass values.

Peptide code No.	Calculated mass (Da)	Observed mass (Da)
Peptide 3	1811.4	1812.4 (M+H) <sup>+</sup> 1834.4(M+Na) <sup>+</sup>
MP5	1750.6	1749.5 (M-H) <sup>-</sup>
MP6	1680.1	1679.4 (M-H) <sup>-</sup>
MP7	1820.3	1819.4 (M-H) <sup>-</sup>
MP8	1724.1	1725.1 (M+H) <sup>+</sup> 1747.4 (M+Na) <sup>+</sup>

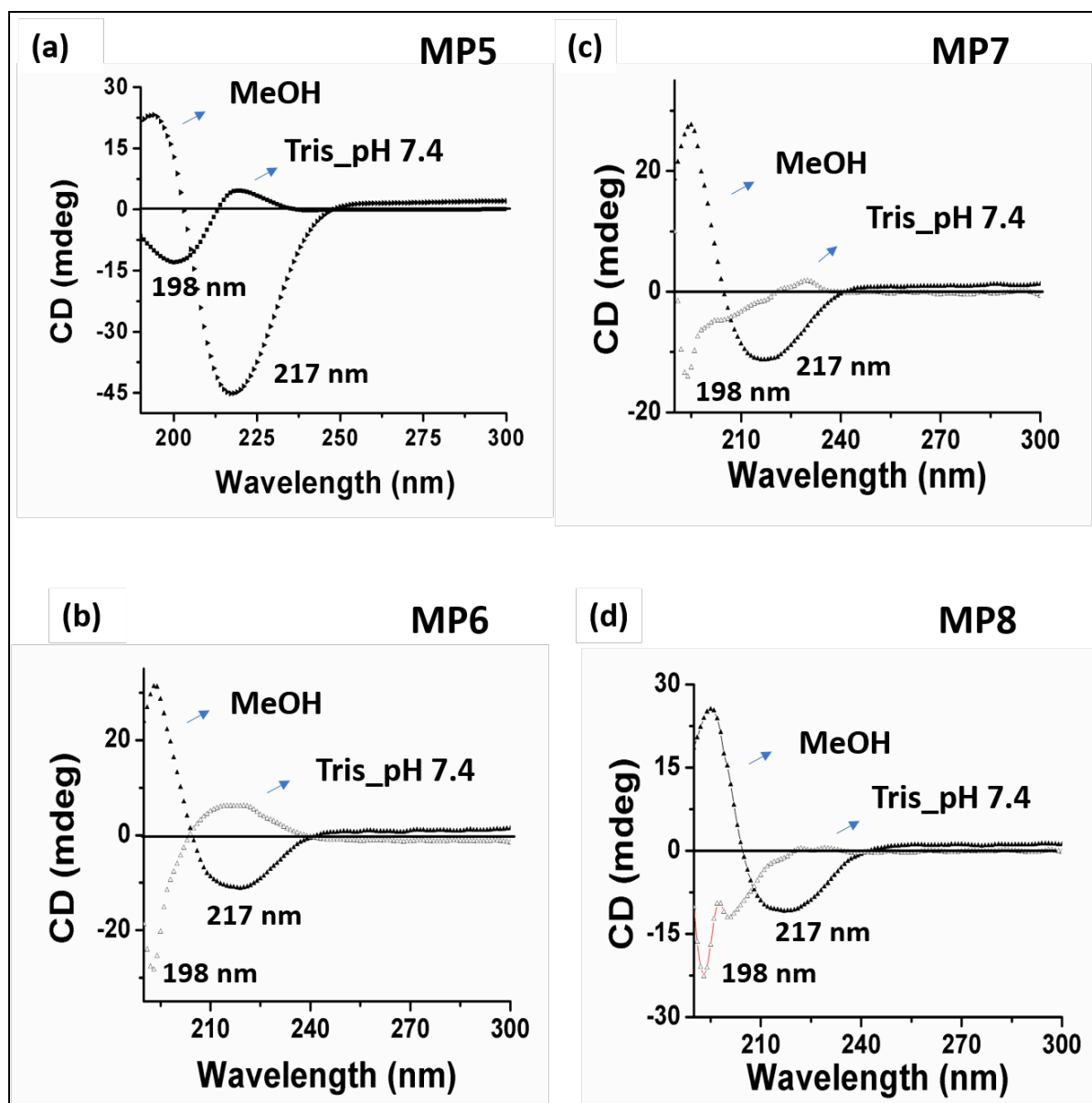


**Figure S2.** (a-d) Circular dichroism spectra of peptides MP5, MP6, MP7 and MP8 in MeOH and 20 mM Tris HCl at pH 7.4. In MeOH, all the four peptides showed beta structure whereas at pH 7.4 these peptides exhibited unstructured conformation.

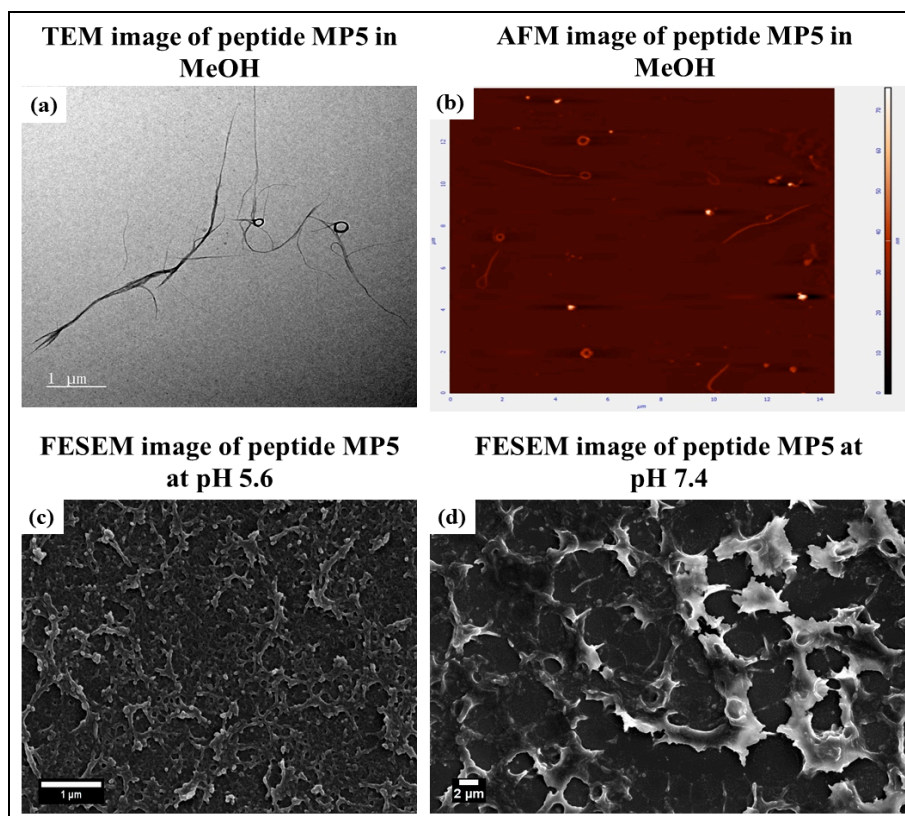


**Figure S3.** (a) TEM (scale bar, 1  $\mu\text{m}$ ) and (b) AFM images of peptide MP5 in MeOH show nanofibrous structure. FE-SEM images of (c) peptide MP5 at pH 5.6 (scale bar, 1  $\mu\text{m}$ ) and (d) peptide MP5 at pH 7.4 (scale bar, 2  $\mu\text{m}$ )

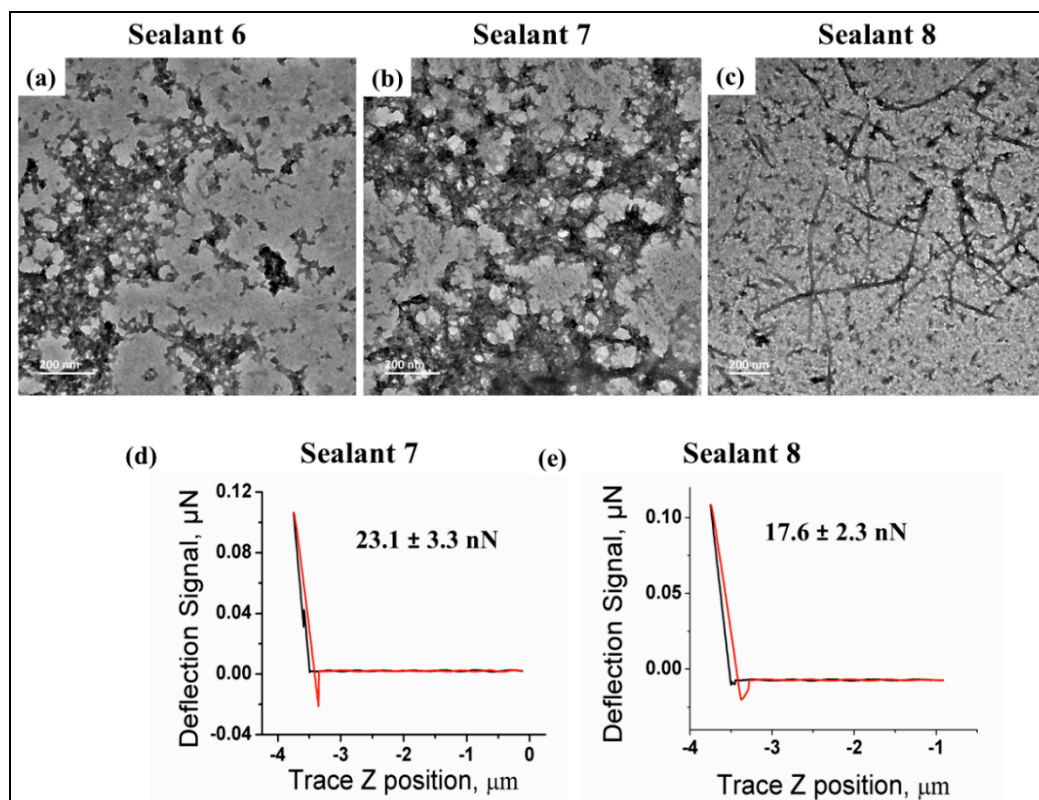


**Figure S4.** TEM images (scale bar, 200 nm) of (a) sealant 6, (b) sealant 7 and (c) sealant 8. Force–distance curves for (d) sealant 7 and (e) sealant 8 obtained by AFM studies and their nanomechanical strength are shown.

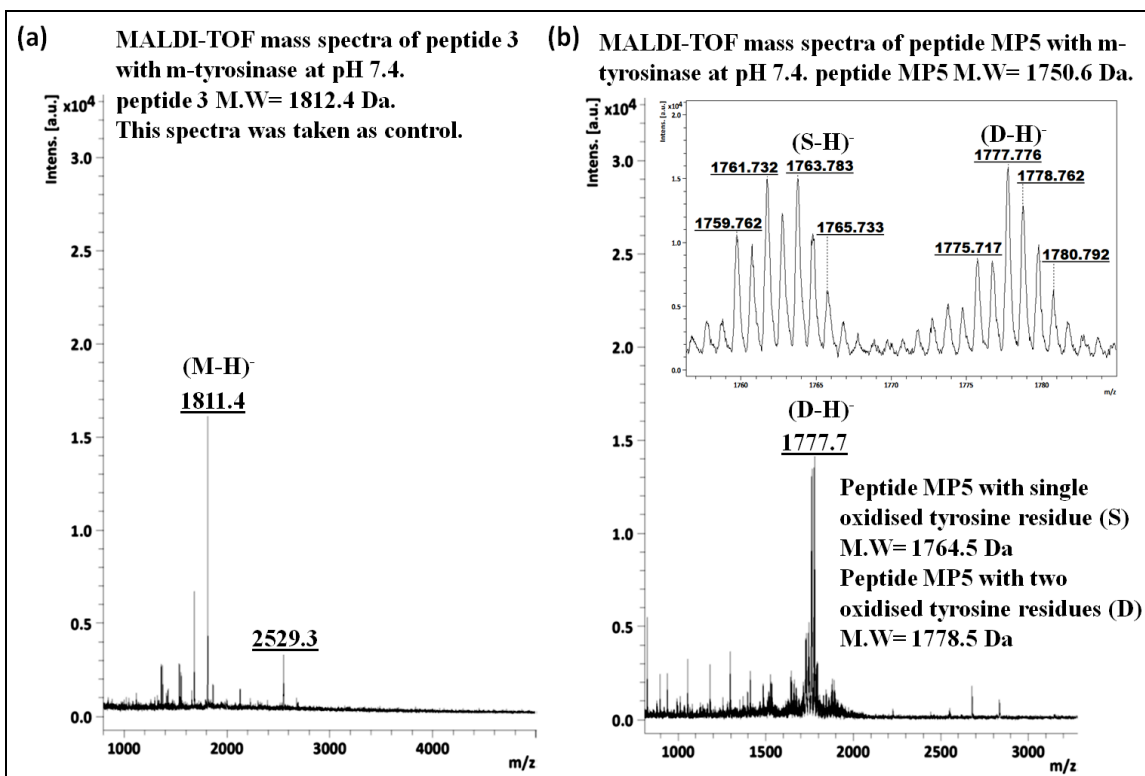


**Figure S5.** (a) MALDI-TOF mass spectra of peptide 3 in presence of mushroom tyrosinase (m-tyrosinase) enzyme at pH 7.4. This spectrum was recorded as control, since sealant 5 contains equimolar mixture of peptide 3 and peptide MP5. (b) MALDI-TOF mass spectra of peptide MP5 in presence of mushroom tyrosinase enzyme at pH 7.4 showed both single tyrosine (1763.7 Da) and double tyrosine oxidation product (1777.7 Da). MALDI-TOF mass spectra were recorded in negative ion mode. This MALDI-TOF mass spectrum was recorded to show tyrosine mediated oxidation of peptide MP5. The single tyrosine oxidation product is represented as “S” and double tyrosine oxidation product is represented as “D”.

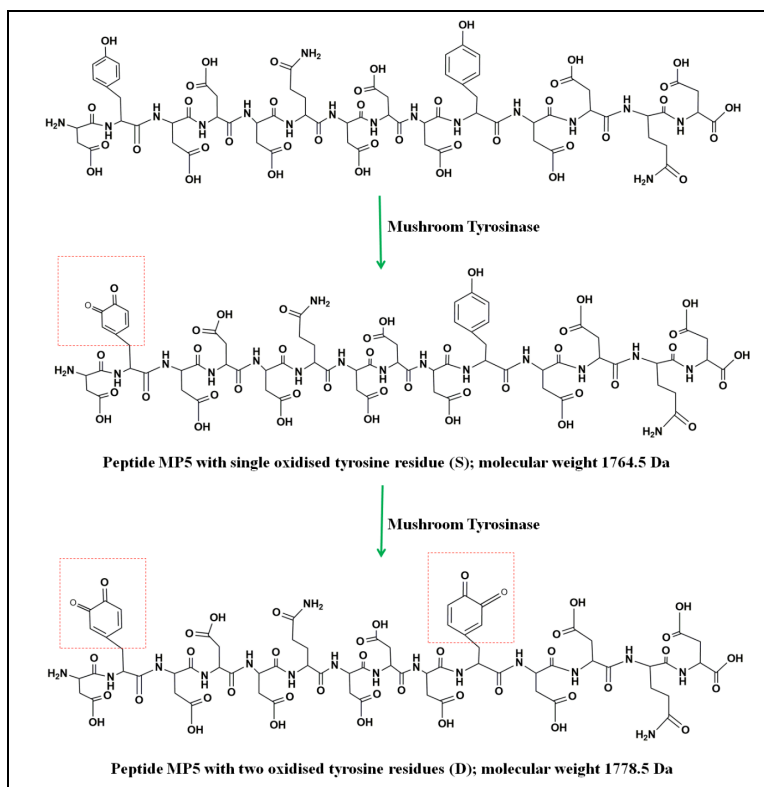


**Figure S6.** Chemical structure of single and double tyrosine oxidation product of peptide MP5.

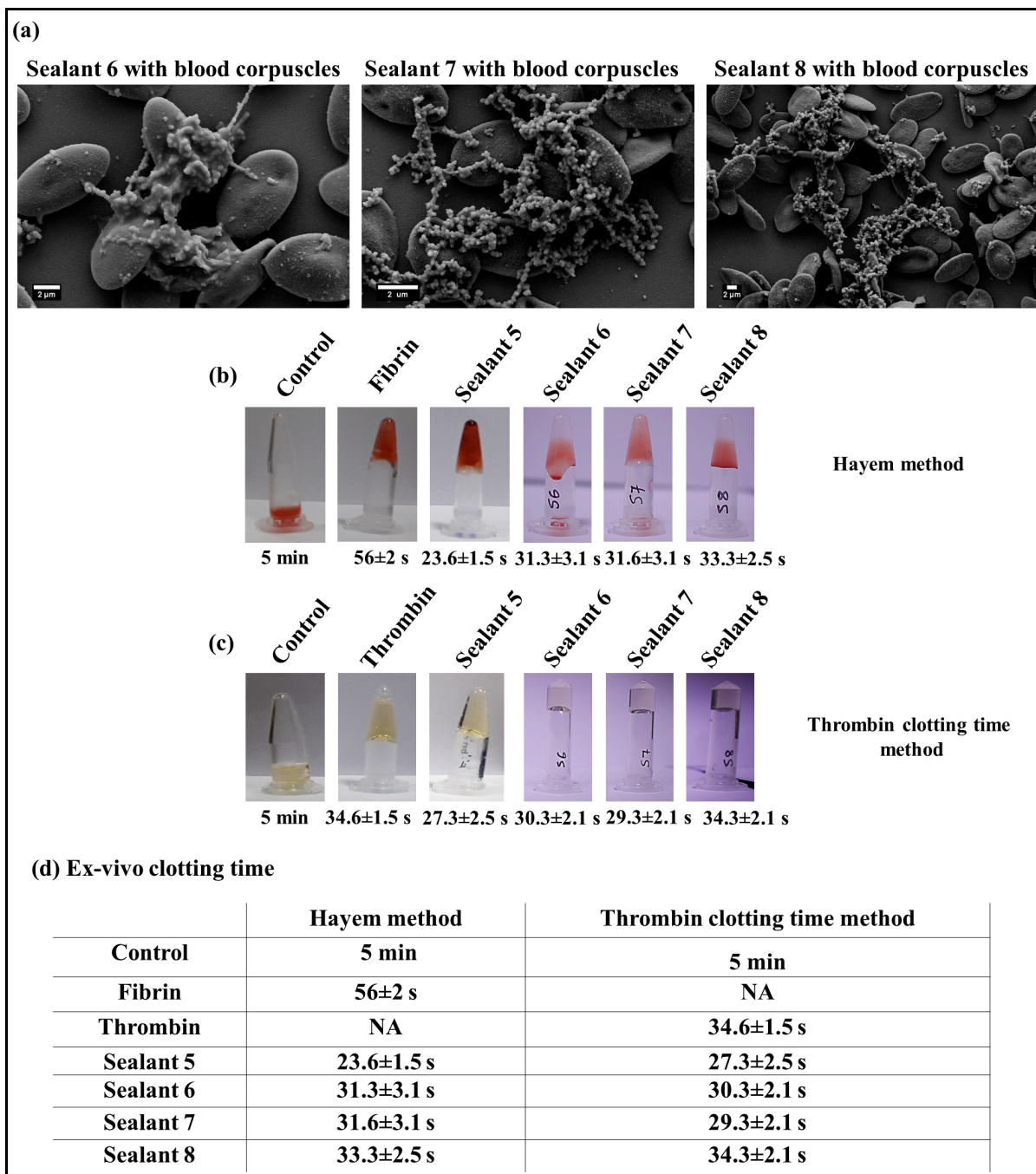


**Figure S7.** FE-SEM images (scale bar, 2  $\mu\text{m}$ ) (a) of sealant 6 with blood corpuscles, sealant 7 with blood corpuscles and sealant 8 with blood corpuscles. FE-SEM images show sealants 6-8 have predominantly failed to entrap the blood corpuscles. Photographic image of (b) *ex-vivo* clotting time of sealants with blood corpuscles by Hayem method or (c) with plasma by thrombin clotting time method. In Hayem method, blood corpuscles were taken in PBS and sealants were added to this solution externally in order to measure the clotting time. (d) Table shows clotting time of blood corpuscles by Hayem method and clotting time of plasma by Thrombin clotting time method. (b-c) Sealants 6-8 exhibit clotting of blood corpuscles by Hayem method and clotting of plasma by Thrombin clotting method. Sealants 6-8 may have minor cross-linked structure, having linkage between Lys and oxidized Tyr side chains, which have facilitated the entrapping of blood corpuscles or clotting the plasma as evident by Hayem method and Thrombin clotting method, whereas the major self-assembled/cross-linked structure may not favour the entrapping of blood corpuscles or clotting of the plasma.<sup>37</sup> In Hayem method, blood corpuscles in PBS was taken as control sample and in Thrombin clotting time method, plasma mixed with 0.15 mL PBS (25 mM PBS buffer, pH 7.4 with 5mM  $\text{CaCl}_2$ ) was taken as control sample.

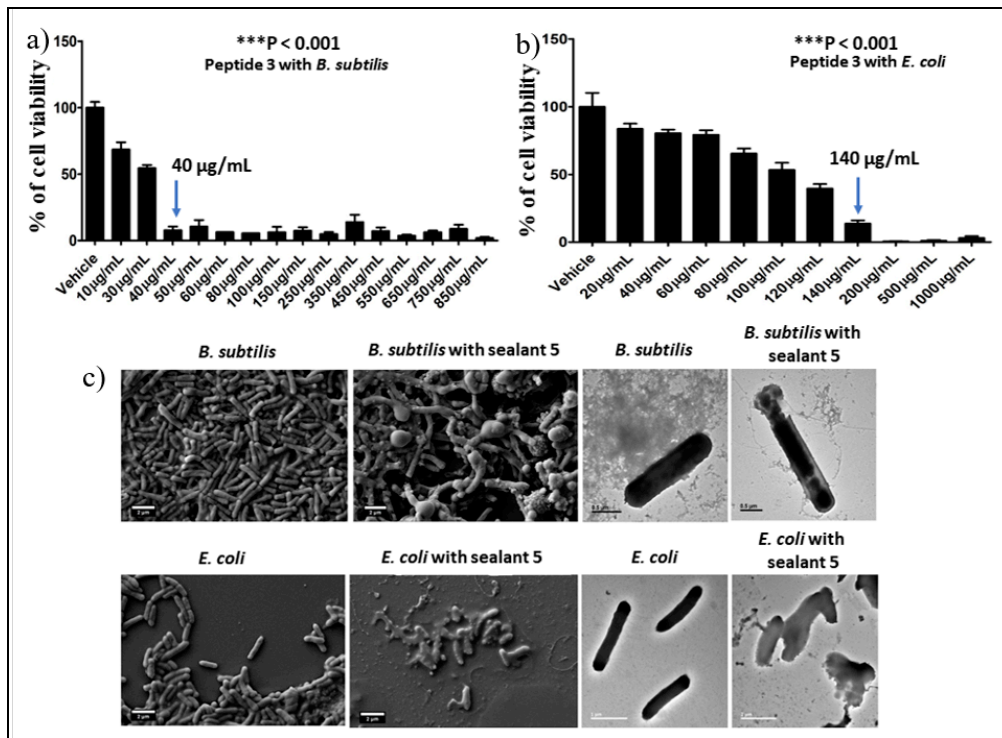


**Figure S8.** Determination of MIC values of peptide 3 against (a) *B. subtilis* and (b) *E. coli*. Data are represented as mean  $\pm$  SEM of  $n=3$  at each data point ( $***p < 0.001$  for all groups compared with control (vehicle)). FE-SEM (scale bar, 2  $\mu\text{m}$ ) and TEM images of (c) *B. subtilis* (scale bar, 0.5  $\mu\text{m}$ ) and (d) *E. coli* against sealant 5 ( $\sim 4$  mM) showed that bacterial outer cell membrane was ruptured due to antibacterial effects of peptide 3. The scale bar for TEM image for *E. coli* was 1  $\mu\text{m}$  and for *E. coli* with sealant 5 was 2  $\mu\text{m}$ .

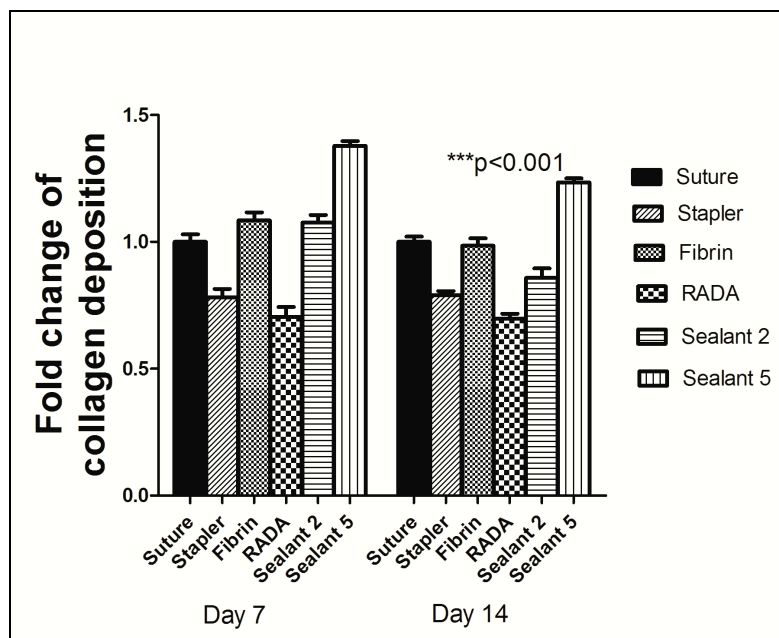


**Figure S9.** Semiquantitative analysis of histology data to determine the fold change of collagen deposition with respect to suture at day 7 and day 14 by the imaging analysis program, ImageJ NIH. The collagen area was estimated by first setting the threshold and then using the area measure mode by limiting to threshold. Data are represented as mean  $\pm$  SEM, of  $n=5$  at each data point ( $***p < 0.001$  for all groups compared with control (suture)).